Supplementary Material (ESI) for PCCP

A New ZnO Nanotetrapods/SnO_2 Nanoparticles Composite Photoanode for High Efficiency Flexible Dye–sensitized Solar Cells

Wei Chen, Yongcai Qiu, and Shihe Yang*

Supplementary Material

Supplementary Material (ESI) for PCCP
This journal is © the Owner Societies 2010

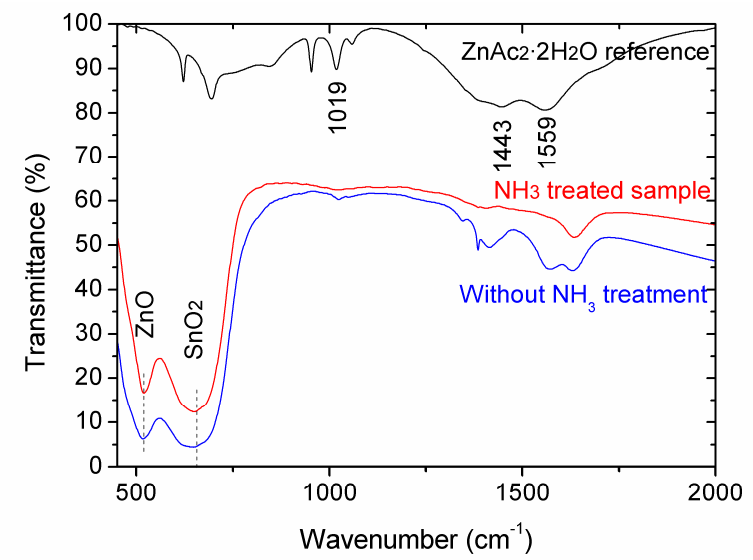

Figure S1. Infra–red spectra of composite films with and without NH_3 treatment, with the top being the spectrum of a $ZnAc_2{\cdot}2H_2O$ reference sample. Peaks associated with carboxylate bands of $ZnAc_2$, the antisymmetric stretch at 1559 cm^{-1}, the symmetric stretch at 1443 cm^{-1}, get smaller evidently due to NH_3 treatment of the composite film, reflecting the elimination of $ZnAc_2$ shell by the treatment. Peaks at 519 and 651 cm^{-1} correspond to stretching bands of crystalline ZnO and SnO_2, respectively, in the composite films.

Supplementary Material (ESI) for PCCP
This journal is © the Owner Societies 2010

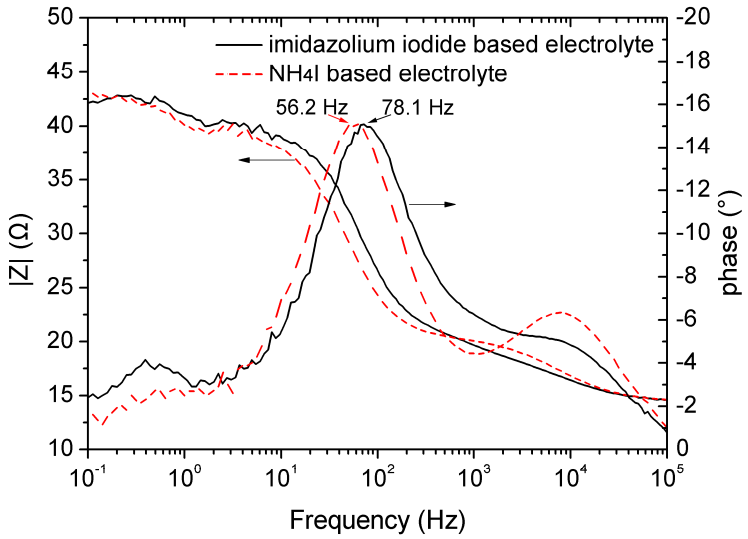

Figure S2. Impedance spectra (Bode plots) of composite photoanode based DSSCs using different electrolytes. The characteristic frequencies (f_r) for recombination process in NH_4I based electrolyte (56.2 Hz) is significantly lower than that in imidazolium iodide based electrolyte (78.1 Hz), which implies much longer recombination time (τ_r) in NH_4I based electrolyte using $\tau_r = 1/(2\pi f_r)$ for calculation.

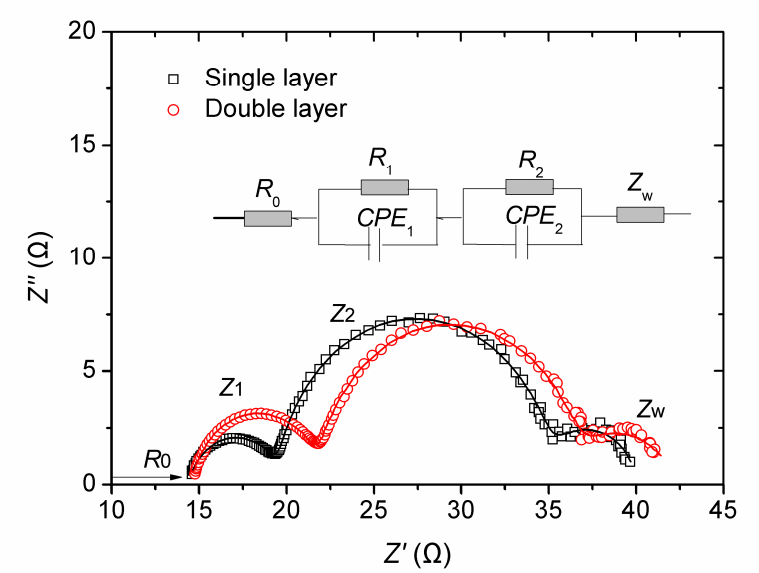

Figure S3. Impedance spectra of a single–layer composite film with a thickness of 10.3 μm (□) and a double–layer–structured film (○) with a 3.3 μm nanotetrapods scattering layer on the top. The inset is a simplified fitting model: R_0 derives from sheet resistance of FTO–coated glass, Z_1 is associated with charge transport at FTO/active film, Pt/electrolyte, and inter–nanostructure interfaces, Z_2 is with respect to charge transport at active film/electrolyte interface, Z_w is Warburg diffusion impedance of electrolyte ions. The fitting lines reveal that R_1 increases from 5.16 to 7.34 Ω and R_2 decreases from 15.6 to 14.7 Ω due to the addition of the light scattering layer. R_1, R_2 contribute to the total series resistance and shunt resistance of the solar cell, respectively.

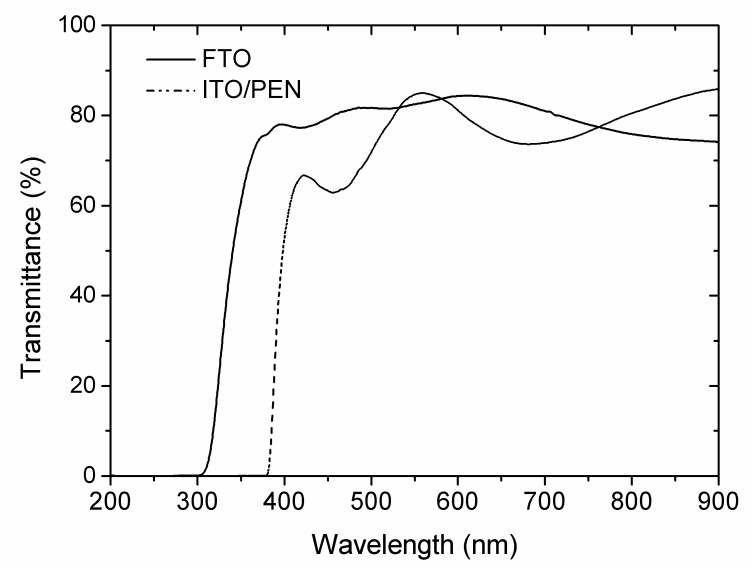

Figure S4. UV–Vis transmittance spectra of FTO–coated glass and ITO/PEN films.

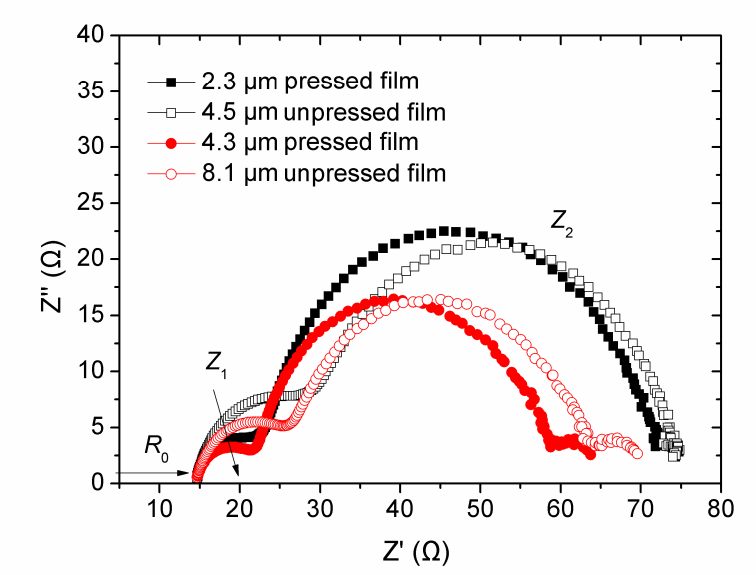

Figure S5. Impedance spectra of the composite films with different thickness. R_1 drops off evidently due to mechanical press, implying a smaller electron transport resistance at the active film/FTO interface and/or the inter–nanostructure interface.

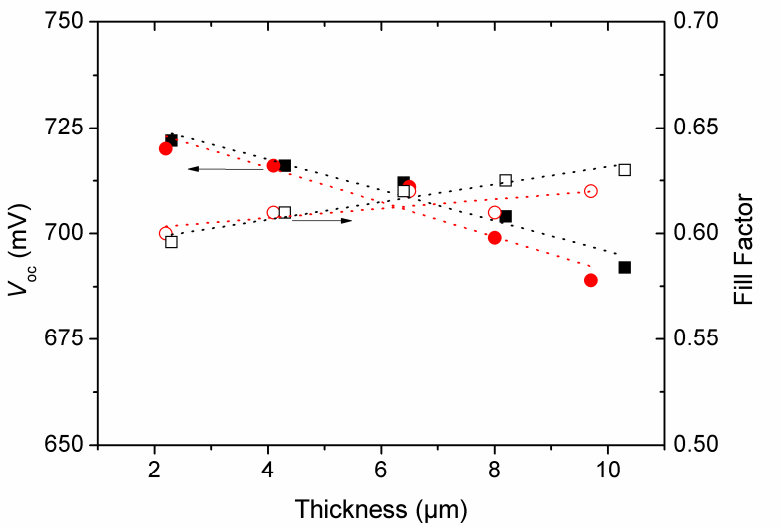

Figure S6. Dependences of V_{oc} (solid symbols) and fill factor (open symbols) on film thickness for composite films with ZnO nanotetrapods (black square symbols) and big particles (red circle symbols) as additives.

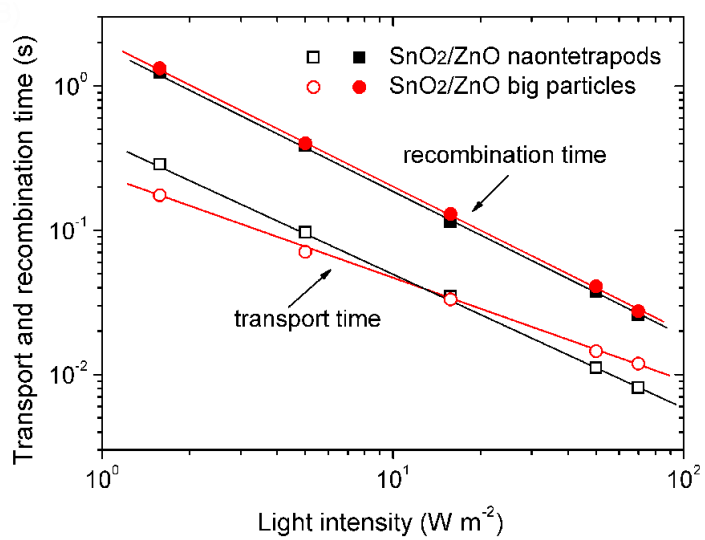

Figure S7. Dependences of electron transport time and recombination time on light intensity for composite films containing ZnO nanotetrapods (black square symbols) and big ZnO particles (red circle symbols) as additives. Similar observation were reported previously in high temperature calcined SnO_2/ZnO nanocomposite films.

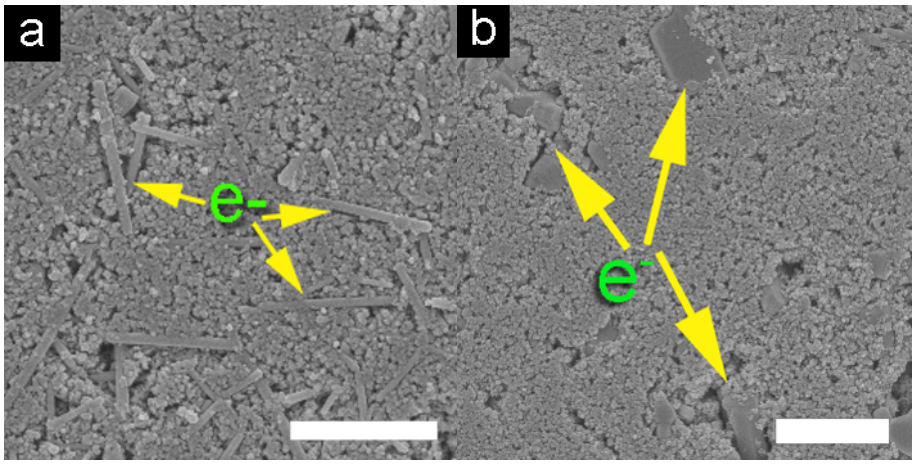

Figure S8. SEM images of composite films containing ZnO nanotetrapods (a) and ZnO big particles (b) as additives. Scale bar = 1 μm. Yellow arrow–lines highlight different lengths the localized electrons have to migrate from SnO_2 nanoparticles to the neighboring ZnO sites.